EUKARYOTIC CELL, Nov. 2010, p. 1755–1765 Vol. 9, No. 11
1535-9778/10/$12.00 doi:10.1128/EC.00029-10

Endosomal and AP-3-Dependent Vacuolar Trafficking Routes Make Additive Contributions to *Candida albicans* Hyphal Growth and Pathogenesis▽†

Glen E. Palmer*

Department of Oral and Craniofacial Biology, Louisiana State University Health Sciences Center, School of Dentistry, 1100 Florida Avenue, New Orleans, Louisiana 70119

Received 3 February 2010/Accepted 14 September 2010

Candida albicans **mutants deficient in vacuolar biogenesis are defective in polarized hyphal growth and virulence. However, the specific vacuolar trafficking routes required for hyphal growth and virulence are unknown. In *Saccharomyces cerevisiae*, two trafficking routes deliver material from the Golgi apparatus to the vacuole. One occurs via the late endosome and is dependent upon Vps21p, while the second bypasses the endosome and requires the AP-3 complex, including Aps3p. To determine the significance of these pathways in *C. albicans* hyphal growth and virulence, *aps3*Δ/Δ, *vps21*Δ/Δ, and *aps3*Δ/Δ *vps21*Δ/Δ mutant strains were constructed. Analysis of vacuolar morphology and localization of the vacuolar protein Mlt1p suggests that *C. albicans* Aps3p and Vps21p mediate two distinct transport pathways. The *vps21*Δ/Δ mutant has a minor reduction in hyphal elongation, while the *aps3*Δ/Δ mutant has no defect in hyphal growth. Interestingly, the *aps3*Δ/Δ *vps21*Δ/Δ double mutant has dramatically reduced hyphal growth. Overexpression of the Ume6p transcriptional activator resulted in constitutive hyphal growth of wild-type, *aps3*Δ/Δ, and *vps21*Δ/Δ strains and formation of highly vacuolated subapical compartments. Thus, Ume6p-dependent transcriptional responses are sufficient to induce subapical vacuolation. However, the *aps3*Δ/Δ *vps21*Δ/Δ mutant formed mainly pseudohyphae that lacked vacuolated compartments. The *aps3*Δ/Δ strain was virulent in a mouse model of disseminated infection; the *vps21*Δ/Δ mutant failed to kill mice but persisted within kidney tissue, while the double mutant was avirulent and cleared from the kidneys. These results suggest that while the AP-3 pathway alone has little impact on hyphal growth or virulence, it is much more significant when endosomal trafficking is disrupted.**

The fungal vacuole is an acidic cellular compartment containing a variety of hydrolytic enzymes. It has a central role in the turnover of cellular macromolecules, is a storage site for many metabolites (24), and is crucial for resistance to osmotic, ionic, pH, and oxidative stresses. A number of previous studies have attempted to define the importance of vacuolar function in pathogenic fungi, including the mucosal and systemic opportunist *Candida albicans*. Several *C. albicans* mutants deficient in vacuolar trafficking have been reported which are sensitive to various stresses and defective in polarized hyphal growth (4, 8, 23, 34, 42). Furthermore, several of these mutants have profound defects in virulence. The vacuole's role in stress tolerance is likely to be crucial for colonization of host tissue and survival of the ensuing immune response. In addition, *C. albicans* virulence requires transition between yeast and highly polarized hyphal modes of growth (28, 39). Thus, the fungal vacuole may act on two levels during infection: to enhance *C. albicans* survival within host tissue and to support polarized hyphal growth required for tissue damage (23, 35). However, the relative contribution of either facet of vacuolar function to pathogenesis is yet to be determined.

During *C. albicans* hyphal growth, the fungal vacuole expands dramatically to produce subapical cells devoid of cytoplasm, while the cytoplasm migrates within the hyphal tip compartment (2, 21). This increase in volume necessitates a significant redistribution of cellular membrane to the subapical vacuoles. However, the mechanism by which subapical vacuoles expand is unknown, as is the mechanism by which vacuolar transport supports polarized hyphal growth. Furthermore, how subapical vacuole expansion is coordinated with apical extension during hyphal growth is unknown. Finally, while several distinct vacuolar trafficking pathways are known to exist (9), the importance of each to *C. albicans* hyphal growth and pathogenesis has not been determined.

Many vacuolar enzymes are delivered via the early stages of the secretory network. In *Saccharomyces cerevisiae*, at least two distinct biosynthetic trafficking routes deliver proteins from the Golgi apparatus to the vacuole (6). One delivers proteins, including carboxypeptidase Y, via a late endosome (also known as the prevacuole compartment [PVC]). This endosomal route is dependent upon the Rab GTPase Vps21p (18). A second pathway sorts cargo, including alkaline phosphatase (ALP), into a distinct set of vesicles which bypass the late endosome and are delivered directly to the vacuole. The ALP trafficking pathway is facilitated by the AP-3 coat complex, which has four subunits (Aps3p, Apm3p, Apl5p, and Apl6p) and functions in the formation of ALP vesicles at the trans-

* Mailing address: Department of Oral and Craniofacial Biology, LSUHSC, School of Dentistry, 1100 Florida Avenue, Box F8-130, New Orleans, LA 70119. Phone: (504) 941-8005. Fax: (504) 941-8319. E-mail: gpalme@lsuhsc.edu.

† Supplemental material for this article may be found at http://ec.asm.org/.

▽ Published ahead of print on 24 September 2010.

TABLE 1. Oligonucleotides used in this study

Primer	Sequence (5′→3′)[a]
APS3DISF	AATGATGGTCTTCCGAGACTAATGAAATTCTATACCAAAGTCGATATTCCAACACAGAAATTGCTCTTGCTGTGGAATTGTGAGCGGATA
APS3DISR	TATACTATTTTTGCATAATTCATTTCGTATTTATCGCTTTTACCTACCCCAGAACCCTCTATCTCGAGACTTTCCCAGTCACGACGTT
APS3AMPF2	TCATCAGAGCTCCTTTGCACCAACAATGGGGGC
APS3AMPR	TCATCAGGATCCAGGAAGCAGAAAGGTTGATGC
APS3PBR	TGCCAGCCAAATACCAAATCC
APS3DETF	AAGATTTGGATGATATCAAGG
APS3DETR	CCTACCCCAGAACCCTCTATCTCG
UME6ORFF	TCATCAGTCGACGTATAAATGATTACCCATATGG
UME6AMPMLUR	TCATCAACGCGTTACGAGAATATTAATGTGTGC
ACT1PF	TCATCAGGTACCCCAGCCTCGTTTATAAACTTAGTC
ACT1PR	TCATCAGTCGACTTTGAATGATTATATTTTTTTAATATTAATATCGAG
MLT1GFPF	ACCTCAAAACTTGTTGAAGAACAAAGACAGTATTTTCTACTCTCTTGCCAAAGAAGGTGGATACATAGATGGTGGTGGTTCTAAAGGTGAAGAATTATT
MLT1GFPR	TGTAAACTAAAAAAAATATTATTGTATAAATAAAAAAATCACTATATGAATATATATCGCACCGATATATATCTAGAAGGACCACCTTTGATT
MLT1DETF	GATCTTAGTGTTAGATAGTGG
ARG4DETF	ATCAATTAACACAGAGATACC
ARG4DETR	CCGAGCTTGGCGTAATCATGG
HIS1F1268	CCGCTACTGTCTCTACTTTG
HIS1DETF	TCATCCTCCAGGATCCCGCGG
URA3INTF	TTAGTGTTACGAATCAATGGC
URA3INTR	CAATTATAAATGTGAAGGGGG
GFPDETR	CATCACCTTCACCTTCACCGG

[a] Engineered restriction enzyme sites are underlined.

Golgi apparatus (12, 40). The purpose of this study was to determine the relative contributions of endosomal and AP-3-dependent trafficking routes to *C. albicans* hyphal growth and virulence.

MATERIALS AND METHODS

Growth conditions. Strains were routinely grown on YPD (1% yeast extract, 2% Bacto peptone, 2% dextrose) at 30°C, supplemented with uridine (50 μg ml^{-1}) when necessary (22). For growth curves, overnight cultures were subcultured into 20 ml fresh YPD medium to an optical density at 600 nm (OD_{600}) of 0.2 and incubated at 30°C with shaking. The OD_{600} was determined from samples taken hourly. Transformants were selected on minimal medium (YNB [6.75 g $liter^{-1}$ yeast nitrogen base plus ammonium sulfate and without amino acids, 2% dextrose, 2% Bacto agar]) supplemented with the appropriate auxotrophic requirements, as described for *S. cerevisiae* (10), or uridine at 50 μg ml^{-1}.

Plasmid construction. Plasmids pGEMURA3, pGEMHIS1, and pRSARGΔSpe (45) were provided by A. Mitchell (Carnegie Mellon University). Plasmid pLUX (38) was provided by W. Fonzi (Georgetown University). Plasmid pLUXVPS21 was previously constructed (23), and pLUXAPS3 was made as follows. The *APS3* open reading frame (ORF) with 5′ and 3′ untranslated region (UTR) sequences was amplified from SC5314 gDNA using HiFi Platinum *Taq* (Invitrogen) and primers APS3AMPF2 and APS3AMPR (Table 1). Purified products were then cloned into the BamHI site of vector pLUX. p*ACT1* was made by amplifying 1,000 bp of the *ACT1* 5′ UTR using primers ACT1PF and ACT1PR with HiFi Taq. The product was then cloned between the KpnI and SalI sites of CIp10 (31). p*ACT1UME6* was made by amplifying the *UME6* ORF and 3′ UTR sequences with UME6ORFF and UME6AMPMLUR primers and cloning downstream of the *ACT1* promoter in p*ACT1*, between the SalI and MluI sites.

Strain construction. Strains used in this study are described in Table 2. Gene deletion strains were constructed by the PCR-based approach described by Wilson et al., using the *ura3*$^-$ *his1*$^-$ *arg4*$^-$ strain BWP17 (45), kindly provided by A. Mitchell (Carnegie Mellon University). *C. albicans* was transformed using the lithium acetate procedure (19). The *vps21*Δ/Δ mutant was constructed in a previous study (23). *APS3* deletion cassettes were amplified by PCR using pARGΔSpe (*ARG4* marker), pGEMHIS1 (*HIS1* marker), or pDDB57 (recyclable *URA3-dpl200* cassette) (44, 45) as a template with the primer pair APS3DISF and APS3DISR. *C. albicans* is diploid; thus sequential deletion of each *APS3* allele was achieved using first *aps3*Δ::*ARG4* and then *aps3*Δ::*HIS1* disruption cassettes to generate a *ura3*$^-$ *aps3*Δ/Δ strain. An *aps3*Δ/Δ *vps21*Δ/Δ double mutant was made by sequentially deleting both *APS3* alleles from a *vps21*Δ/Δ *ura3*$^-$ *arg4*$^-$ strain previously constructed (23). This strain was transformed with the *aps3*Δ::*URA3-dpl200* cassette and then the *aps3*Δ::*ARG4* cassette. The regeneration of *ura3*$^-$ recombinants was selected on YNB medium supplemented with uridine and 1 μg ml^{-1} 5-fluoroorotic acid (5-FOA) (5). Correct integration of either cassette was confirmed at each step by diagnostic PCR using primers ARG4DET2 plus APS3AMPR (*ARG4* integration), HIS1F1268 plus APS3AMPF (*HIS1* integration), or URA3-5 plus APS3AMPF (*URA3* integration). Southern blot analysis was also performed using a specific probe to the 5′ UTR of *APS3*, amplified using primers APS3AMPF plus APS3PBR. Correct gene deletion resulted in replacement of the entire 480-bp *APS3* ORF. Finally a wild-type copy of *APS3* or *VPS21*, including 5′ and 3′ flanking sequences, was introduced to the deletion strains on pLUXAPS3 or pLUXVPS21 (23) to produce prototrophic "reconstituted" strains. Prototrophic gene deletion strains were produced by transforming the mutant strains with plasmid vector (pLUX) alone. Either plasmid was digested with NheI to target integration into (and reconstitute) the *URA3* loci. This strategy circumvents the well-described positional effects of *URA3* integration (26).

Plasmids harboring wild-type (pEM-31) or "dominant active" (pEM16-1 and pEM16-3) *RIM101* alleles (15) were linearized with HpaI to target integration into the *RIM101* locus; *ura3*$^-$ recipient strains were transformed, and Ura$^+$ transformants were selected. p*ACT1UME6* was linearized with either StuI to target integration into the RP10 locus or PstI to target integration into the endogenous *UME6* locus. Ura$^+$ transformants were then selected. *MLT1* was genomically tagged using the approach of Gerami-Nejad et al. (17). Megaprimers MLT1GFPF and MLT1GFPR were used to amplify a *GFP-URA3* cassette from pGFP-URA3, with flanking sequences to target in-frame integration at the 3′ end of the *MLT1* ORF; *ura3*$^-$ recipient strains were transformed with this cassette. Correct integration was confirmed by PCR from genomic DNA using primers MLT1DETF and GFPDETR2.

Stress phenotypes. *C. albicans* strains were grown overnight in YPD broth at 30°C, cell density was adjusted to 10^7 ml^{-1} in sterile water, and serial 1:5 dilutions were performed in a 96-well plate. Cells were then applied to agar using a sterile multipronged applicator. Resistance to temperature stress was determined on YPD agar at 37 and 42°C, and resistance to osmotic stress was determined on YPD agar plus 2.5 M glycerol or 1.5 M NaCl. Other stresses included YPD plus 5 mM caffeine, 10 nM rapamycin, 5 mM sodium orthovana-

TABLE 2. *C. albicans* strains used in this study

Strain	Relevant genotype	Source or reference
SC5314	*VPS21/VPS21 APS3/APS3*	20
YJB6284	*VPS21/VPS21 APS3/APS3*	3
BWP17	*VPS21/VPS21 APS3/APS3 ura3*Δ/Δ *his1*Δ/Δ *arg4*Δ/Δ	45
CAI4	*VPS21/VPS21 APS3/APS3 ura3*Δ/Δ	21
APD1/2	*ura3*Δ/Δ::*URA3 his1*Δ/Δ *arg4*Δ/Δ *aps3*Δ::*ARG4/aps3*Δ::*HIS1*	This study
APR1/3	*ura3*Δ/Δ::*URA3*::*APS3 his1*Δ/Δ *arg4*Δ/Δ *aps3*Δ::*ARG4/aps3*Δ::*HIS1*	This study
21F1	*vps21*Δ::*HIS1/vps21*Δ::*dpl200 APS3/APS3 ura3*Δ/Δ *arg4*Δ/Δ	23
VD1/4	*ura3*Δ/Δ::*URA3 his1*Δ/Δ *arg4*Δ/Δ *vps21*Δ::*ARG4/vps21*Δ::*HIS1*	23
VR1/4	*ura3*Δ/Δ::*URA3*::*VPS21 his1*Δ/Δ *arg4*Δ/Δ *vps21*Δ::*ARG4/vps21*Δ::*HIS1*	23
213L2/21	*ura3*Δ/Δ::*URA3 his1*Δ/Δ *arg4*Δ/Δ *vps21*Δ::*dpl200/vps21*Δ::*HIS1aps3*Δ::*dpl200/aps3*Δ::*ARG4*	This study
213A2/21	*ura3*Δ/Δ*URA3*::*APS3 his1*Δ/Δ *arg4*Δ/Δ *vps21*Δ::*dpl200/vps21*Δ::*HIS1aps3*Δ::*dpl200/aps3*Δ::*ARG4*	This study
213V3/21	*ura3*Δ/Δ*URA3*::*VPS21 his1*Δ/Δ *arg4*Δ/Δ *vps21*Δ::*dpl200/vps21*Δ::*HIS1aps3*Δ::*dpl200/aps3*Δ::*ARG4*	This study
CU1-3	*ura3*Δ/Δ *UME6/UME6*::*ACT1-UME6*::*URA3*	This study
AU1-3	*ura3*Δ/Δ *his1*Δ/Δ *arg4*Δ/Δ *aps3*Δ::*ARG4/aps3*Δ::*HIS1 UME6/UME6*::*ACT1-UME6*::*URA3*	This study
VU1-3	*ura3*Δ/Δ *his1*Δ/Δ *arg4*Δ/Δ *vps21*Δ::*ARG4/vps21*Δ::*HIS1 UME6/UME6*::*ACT1-UME6*::*URA3*	This study
AVU1-3	*ura3*Δ/Δ *his1*Δ/Δ *arg4*Δ/Δ *vps21*Δ::*dpl200/vps21*Δ::*HIS1aps3*Δ::*dpl200/aps3*Δ::*ARG4 UME6/UME6*::*ACT1-UME6*::*URA3*	This study
CRM1-3	*ura3*Δ/Δ *MLT1/MLT1-GFP*::*URA3*	This study
ARM1-3	*ura3*Δ/Δ *his1*Δ/Δ *arg4*Δ/Δ *aps3*Δ::*ARG4/aps3*Δ::*HIS1 MLT1/MLT1-GFP*::*URA3*	This study
VRM1-3	*ura3*Δ/Δ *his1*Δ/Δ *arg4*Δ/Δ *vps21*Δ::*ARG4/vps21*Δ::*HIS1 MLT1/MLT1-GFP*::*URA3*	This study
AVRM1-3	*ura3*Δ/Δ *his1*Δ/Δ *arg4*Δ/Δ *vps21*Δ::*dpl200/vps21*Δ::*HIS1aps3*Δ::*dpl200/aps3*Δ::*ARG4 MLT1/MLT1-GFP*::*URA3*	This study

date, 200 μg ml^{-1} Congo red, and 0.05% SDS. Carbon source utilization was tested using 3% ethanol, glycerol, or potassium acetate instead of glucose. Secreted protease activity was examined on bovine serum albumin (BSA) plus YE agar at 37°C (13). Resistance to nitrogen starvation was determined in SD-N medium (32), and viability was determined at time intervals as CFU counts on YPD agar.

Morphogenesis assays. Filamentous growth was assessed on M199 (pH 7.5) and 10% fetal bovine serum (FBS) agar (36). Cells from overnight cultures were washed twice, and 10% FBS or M199 liquid medium was inoculated with 10^6 cells ml^{-1} and incubated at 37°C. Samples were examined microscopically at intervals and scored according to the morphology index (MI) described by Odds and colleagues (29, 33). Filamentous growth was also stimulated by sandwiching *C. albicans* cells between two layers of YPD agar (7).

Fluorescence microscopy and localization. Vacuole morphology was assessed by pulse-labeling cells with the fluorescent dye FM4-64 (43) for 20 min and chasing in fresh YPD medium for 2 h (or 3 h for the *ACT1-UME6* strains). Labeled compartments were observed using a deconvolution fluorescence microscope with a tetramethyl rhodamine isocyanate (TRITC) filter set. For colocalization of the Mlt1-green fluorescent protein (GFP) fusion protein, a fluorescein isothiocyanate (FITC) filter set was also used.

Alkaline phosphatase assay. Each strain was grown in YPD at 30°C overnight, and 5×10^8 cells were harvested. Cell extracts were prepared using glass bead breakage, and ALP activity in the supernatant was determined using 4-nitrophenylphosphate as a substrate, to a final concentration of 0.8 mg ml^{-1}, as previously described (16). After a 30-min incubation at 37°C, the reaction was stopped with 100 mM NaOH and the OD_{405} was determined. Controls included minus-extract and minus-substrate reactions.

Mouse model of hematogenously disseminated candidiasis. All procedures were approved by the Institutional Animal Care and Usage Committee of LSUHSC-New Orleans and complied with all relevant federal guidelines. *C. albicans* was grown overnight in YPD cultures at 30°C (200 rpm). Cells were washed twice in sterile PBS, and cell density was determined using a hemocytometer. Each strain was then diluted to 5×10^6 cells ml^{-1} in sterile PBS. Then, 0.1 ml of each cell suspension was inoculated into the lateral tail vein of BALB/c mice (Charles River Laboratories, Maryland). Viable cell counts of each inoculum were confirmed by plating appropriate dilutions onto YPD agar plates and counting the colonies formed after 48 h. Mice were monitored for 28 days, and those showing distress were euthanized. Kaplan-Meier survival curves were plotted, and statistical significance was determined using the log rank test. At day 28, surviving mice were euthanized. The kidneys from each mouse were weighed and homogenized in PBS, and serial dilutions of homogenate were plated to YPD agar. The number of colonies on each plate was determined after 48 h, and the CFU g^{-1} of tissue were calculated.

RESULTS

Identification of *Candida albicans* AP-3 orthologs. BLAST searches of the CGD database identified homologs of all four *S. cerevisiae* AP-3 subunits. The most highly conserved was the small subunit encoded by *APS3*, which was 57% identical to ScAps3p. In order to determine if *C. albicans* possesses a functional AP-3 pathway, *aps3*Δ/Δ deletion and *aps3*Δ/Δ plus *APS3* "reconstituted" strains were constructed. In *S. cerevisiae*, ALP, as well as the vacuolar t-SNARE Vam3p, is delivered to the vacuole through the AP-3 pathway. However, it has been shown that when AP-3-dependent transport is blocked, both Vam3p and ALP still reach the vacuole, as they are redirected into the Vps21p-dependent endosomal trafficking route (12). An *aps3*Δ/Δ *vps21*Δ/Δ double mutant was therefore constructed to determine if there is a functional interaction between Aps3p- and Vps21p-dependent pathways in *C. albicans*. Previous work has established that some mutants with severe vacuolar defects are profoundly affected in growth (23, 35). However, the *aps3*Δ/Δ, *vps21*Δ/Δ, and *aps3*Δ/Δ *vps21*Δ/Δ mutants have growth rates comparable to that of the control strain YJB6284 (see the supplemental material). Furthermore, no defects were observed in utilizing the nonfermentable carbon sources ethanol and glycerol (data not shown).

***C. albicans APS3* functions in vacuolar trafficking.** Vacuolar morphology was examined using the lipophilic dye FM4-64, which is internalized via endocytosis and accumulates within the vacuole (43). The *aps3*Δ/Δ mutant had normal-sized vacuoles but with striking morphological differences from the control strain. Large vesicles accumulated within the vacuole lumens of 32% (n = 150) of *aps3*Δ/Δ cells (Fig. 1A). This morphology was not observed in YJB6284, the reconstituted strain, or *vps21*Δ/Δ mutant cells. As previously reported (23), the *vps21*Δ/Δ mutant exhibited a delayed internalization of FM4-64 from the cell surface but otherwise had a normal vacuole morphology. Surprisingly, the *aps3*Δ/Δ *vps21*Δ/Δ mu-

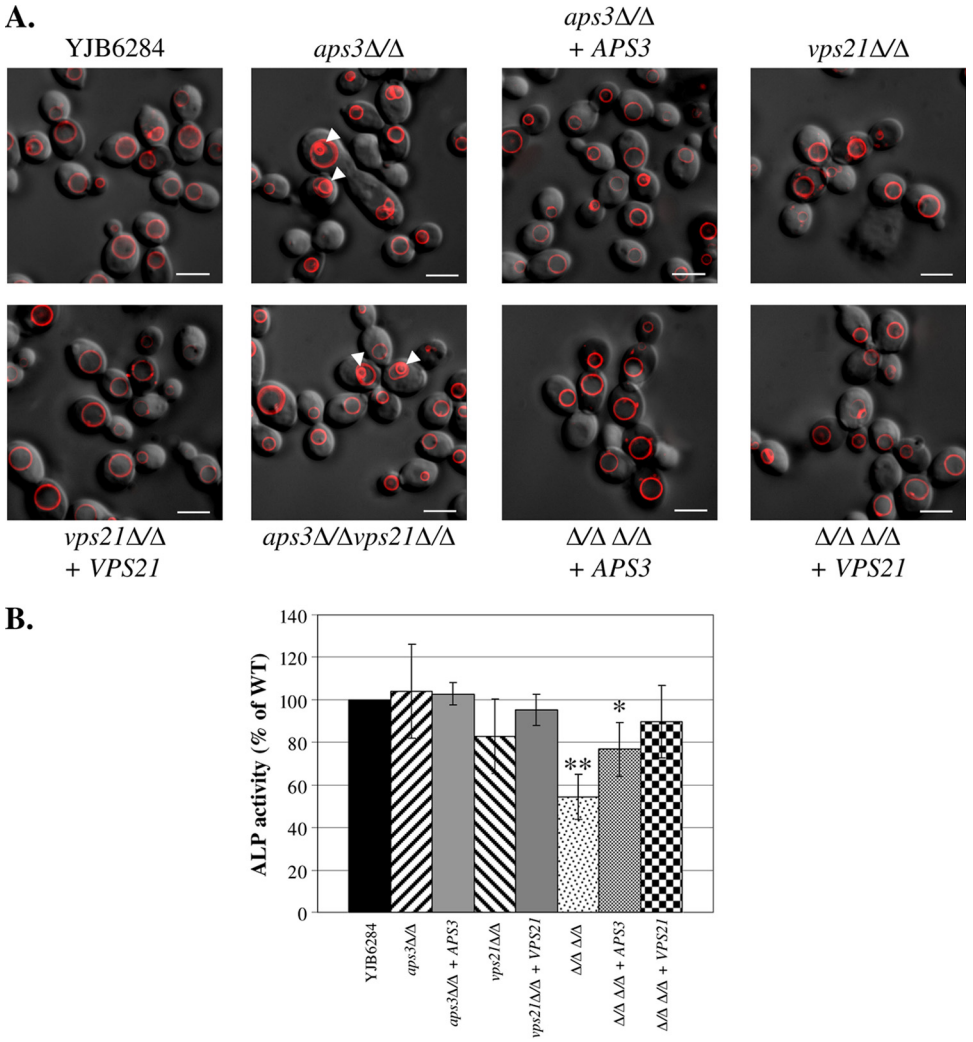

FIG. 1. *C. albicans* Aps3p and Vps21p facilitate distinct vacuolar trafficking pathways. (A) Each strain was pulse-labeled with the endocytic marker FM4-64 and chased for 2 h in fresh medium at 30°C. Cells were then observed by deconvolution fluorescence microscopy to see FM4-64 (red) and Nomarski optics; merged images are shown. Arrowheads indicate internal vesicles within the vacuole lumens of *aps3*Δ/Δ and *aps3*Δ/Δ*vps21*Δ/Δ cells. Scale bar, 5 μM. (B) ALP activity was assayed from cell extracts of each strain and expressed as a percentage of control strain (YJB6284) activity. Results presented are the means and standard deviations of results of three independent experiments. *, $P < 0.05$; **, $P < 0.0001$. WT, wild type.

tant also had large intact vacuoles but exhibited the same morphological defects described for the *aps3*Δ/Δ mutant. As expected, reintroduction of *APS3* (but not *VPS21*) into the double mutant resolved these defects. The *aps3*Δ/Δ *vps21*Δ/Δ mutant also had a delay in dye internalization, which was restored by reintroduction of *VPS21* but not *APS3*. This clearly established that *C. albicans APS3* is involved in vacuolar membrane transport and that its functions are distinct from those of *VPS21*.

In *S. cerevisiae*, ALP is delivered to the vacuole as an inactive precursor, which is proteolytically activated upon delivery to the vacuole (24). In order to assess ALP trafficking in the *aps3*Δ/Δ and *vps21*Δ/Δ mutant strains, ALP activity was assayed. While neither single mutant was significantly affected, the *aps3*Δ/Δ *vps21*Δ/Δ mutant had reduced ALP activity compared to that of the control strain YJB6284 (Fig. 1B). ALP activity was also largely restored by reintroduction of either *APS3* or *VPS21* to the double mutant. This is consistent with ALP trafficking in *S. cerevisiae*, where ALP can transit to the vacuole through either AP-3- or *VPS21*-dependent pathways.

We also examined the localization of an Mlt1-GFP fusion protein, previously localized to the vacuolar membrane (41), in each mutant. In "wild-type" cells, Mlt1-GFP colocalized with FM4-64 in large ring structures, as expected for a vacuolar membrane protein (Fig. 2). Both *aps3*Δ/Δ and *vps21*Δ/Δ mutants showed largely similar distributions, indicating that the fusion protein reached the vacuole, except that the *aps3*Δ/Δ mutant also had significant Mlt1-GFP localization to the previously noted intravacuolar vesicles. In the *aps3*Δ/Δ *vps21*Δ/Δ double mutant, Mlt1-GFP colocalized with FM4-64 on the vacuole, but significant amounts were also mislocalized within the cytoplasm as punctate spots and a diffuse "halo" surrounding the vacuole. These data are consistent with *APS3* and *VPS21* functioning in two independent trafficking pathways to the vacuole, with the Mlt1-GFP cargo being able to utilize

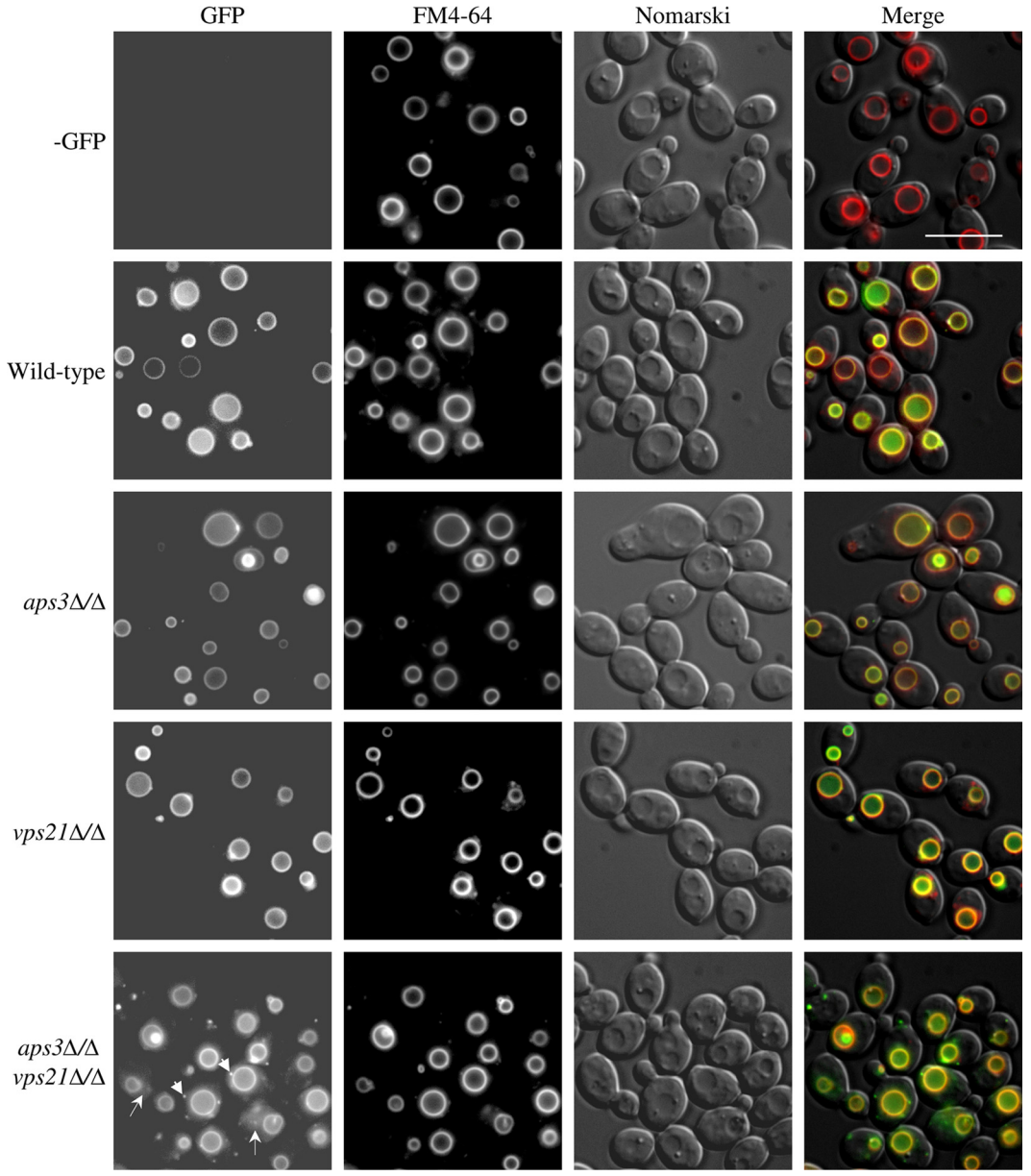

FIG. 2. Mlt1-GFP can transit to the vacuole by either Aps3p- or Vps21p-dependent pathways. An *MLT1-GFP* fusion was introduced into control, *aps3*Δ/Δ, *vps21*Δ/Δ, or *aps3*Δ/Δ *vps21*Δ/Δ strain backgrounds. Each strain was pulse-labeled with FM4-64 to label the vacuole. Cells were then observed by deconvolution fluorescence microscopy to determine Mlt1-GFP (left panel) and FM4-64 (center left) distribution and by Nomarski optics (center right). Merged images are also shown (right panel). Arrowheads indicate punctate Mlt1-GFP, and arrows indicate diffuse cytoplasmic Mlt1-GFP distributions in the double-mutant strain. Scale bar, 10 μM.

either. It also suggests that Mlt1-GFP is able to utilize a third delivery pathway to reach the vacuole when the Aps3p and Vps21p pathways are blocked.

As previously reported, the *vps21*Δ/Δ mutant had increased secreted protease activity compared to the control strains (23), while loss of *APS3* had no impact on this phenotype (data not shown).

AP-3- and *VPS21*-dependent pathways play distinct roles in resisting cellular stress. The fungal vacuole has established roles in resisting cellular stress. Therefore, to determine the biological significance of AP-3 trafficking in *C. albicans*, resistance of each mutant to various cellular stresses was examined. Both single mutants were sensitive to rapamycin, with the double mutant even more sensitive, suggesting that each pathway makes an independent contribution to rapamycin resistance. The *aps3*Δ/Δ mutant seems otherwise unaffected in stress tolerance. No growth defects were observed at 37°C for either mutant strain, and both single mutants grew at 42°C. However, the double mutant showed a synthetic growth defect at 42°C (Fig. 3A), under ionic stress (1.5 M NaCl), and in the presence of caffeine. The *vps21*Δ/Δ mutant was also found to be hypersensitive to Congo red and SDS, agents known to disrupt cell wall integrity. However, loss of *APS3* had no impact on the sensitivity to these agents. Interestingly, the

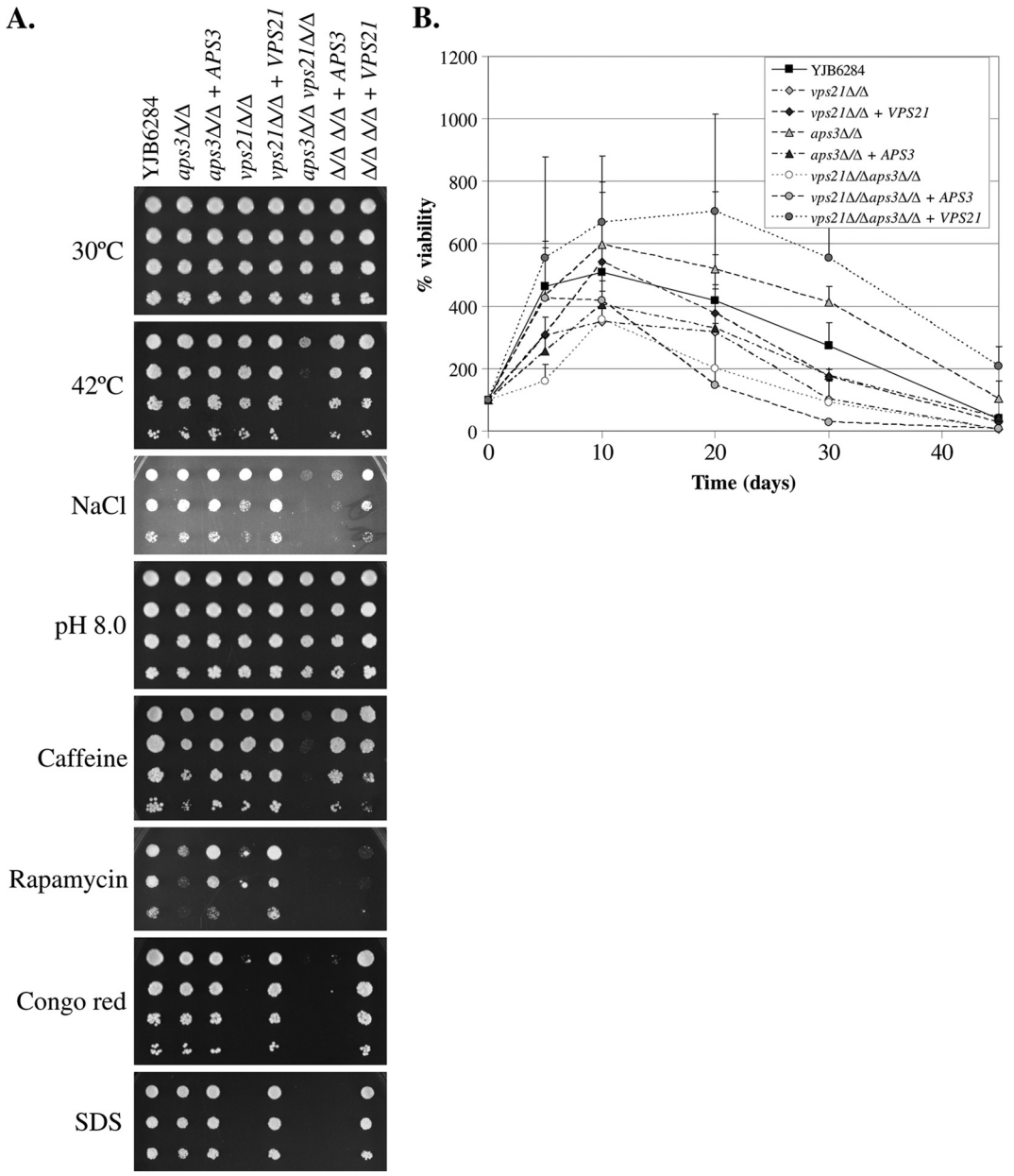

FIG. 3. Loss of both *APS3* and *VPS21* leads to synthetic stress phenotypes. (A) Cell suspensions of each strain were prepared by serial dilution and applied to YPD agar and incubated at 30 or 42°C or to YPD agar supplemented with 1.5 M NaCl, 5 mM caffeine, 10 nM rapamycin, 200 μM Congo red, or 0.05% SDS or at a pH of 8 and incubated at 30°C. (B) To determine resistance to nitrogen starvation, each strain was incubated in SD-N medium. Cell viability was determined as CFU counts from samples taken at intervals and expressed as a percentage of CFU at time zero. Data shown are the means and standard deviations of results of three independent experiments.

*aps3*Δ/Δ mutant was consistently more resistant to nitrogen starvation than the wild-type control strain (Fig. 3B). The *vps21*Δ/Δ mutant was slightly sensitive to nitrogen starvation, as was the *aps3*Δ/Δ *vps21*Δ/Δ mutant. Thus, while loss of *APS3* alone has little effect on stress resistance, the synthetic stress phenotypes of the *aps3*Δ/Δ *vps21*Δ/Δ mutant suggest that there is some functional interplay between AP-3 and endosomal trafficking routes.

AP-3- and *VPS21*-dependent pathways make an additive contribution in supporting hyphal growth. Loss of *APS3* alone has no obvious effect on *C. albicans* hyphal growth on M199/FBS agar, in liquid M199 or FBS culture, or under embedded conditions (Fig. 4). The *vps21*Δ/Δ mutant was previously shown to have mild defects in hyphal growth under each of these conditions (23). However, the double mutant has profound defects in hyphal growth. The double mutant was unable to produce filaments on M199 or FBS agar and formed few filaments when embedded in an agar matrix (Fig. 4A and D). In liquid M199 and FBS media the double mutant grew mainly as yeast and pseudohyphae, with half of the pseudohyphae having an elongated "hook" shape (Fig. 4B and C). Reintroduction of *VPS21* almost completely restored normal hyphal growth un-

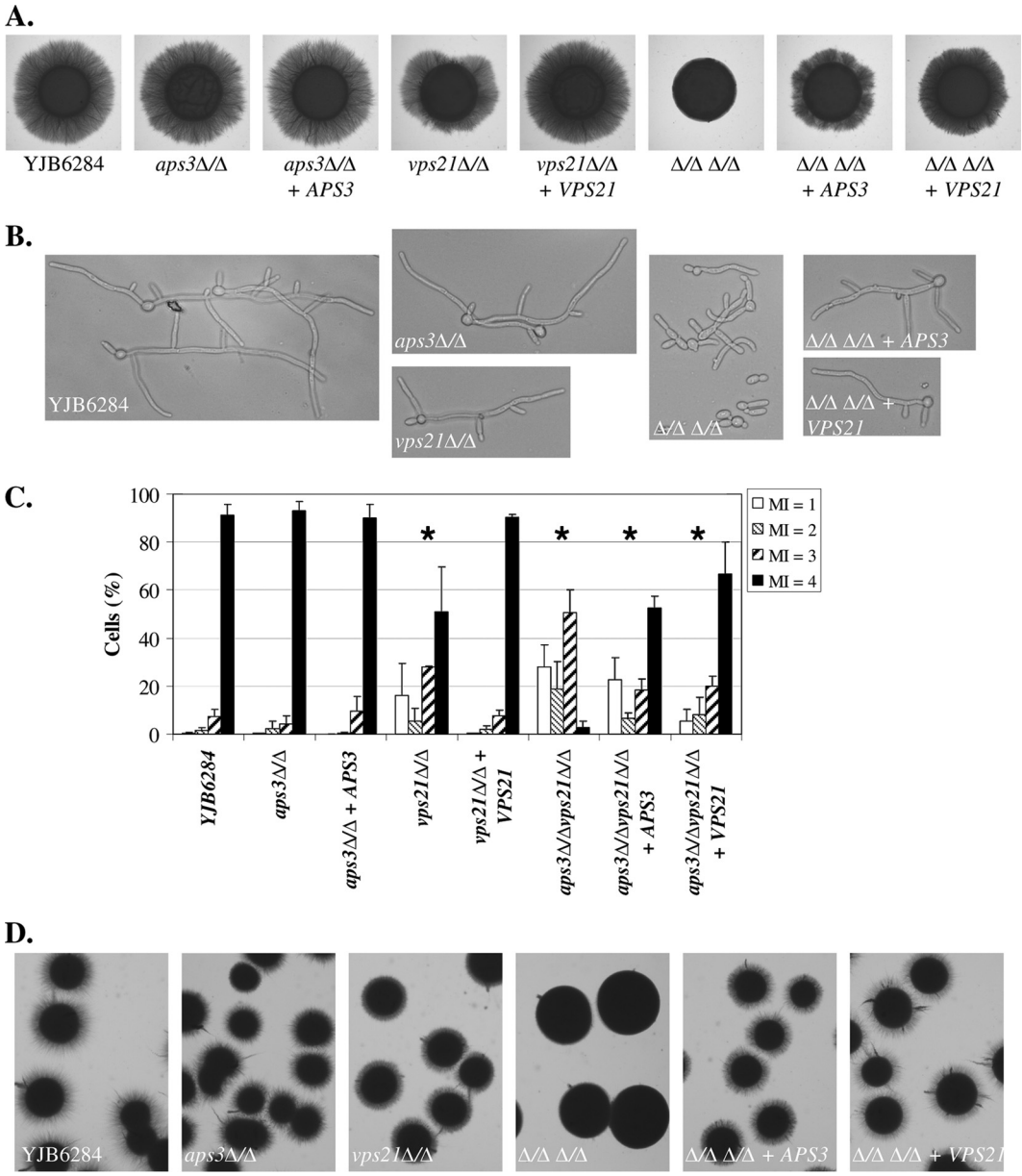

FIG. 4. Aps3p- and Vps21p-dependent pathways make additive contributions to polarized hyphal growth. (A) Cell suspensions of each strain were applied as spots to M199 agar and incubated at 37°C for 4 days. (B) Each strain was induced to filament in 10% FBS at 37°C for 5 h. (C) A minimum of 200 cells grown in FBS at 37°C for 5 h were scored for each strain, according to the morphology index (MI) described by Odds and colleagues (29, 33). MI of 1, spherical and nearly spherical cells; MI of 2, ovoid cells with length up to twice the cell width; MI of 3, pseudohyphal cells with obvious constrictions; MI of 4, parallel-sided true hyphal cells. Data are the means of results of three separate experiments; error bars represent standard deviations. Pearson's chi-square test was used to determine whether the proportion of MI categories observed differed between the control strain (YJB6284) and each of the other strains. *, $P < 0.001$. (D) Cells of each strain were sandwiched between two layers of YPD agar and incubated at room temperature for 3 days.

der each of these conditions, while reintroduction of *APS3* restored hyphal growth to *vps21*Δ/Δ levels. These data imply that AP-3 trafficking becomes much more important in supporting hyphal growth when Vps21p-mediated trafficking is disrupted.

The elongated pseudohyphal cells observed under hypha-inducing conditions could indicate that the double mutant is unable to maintain the highly polarized cell state necessary for true hyphal growth. *UME6* encodes a transcription factor required to maintain polarized hyphal growth and hypha-specific gene transcription (1). Overexpression of *UME6* has been shown to promote extended hyphal growth, even under conditions which would normally support growth in the yeast form (11). To examine the relationship between *APS3*- and *VPS21*-mediated trafficking and the control of hyphal extension, *UME6* was overexpressed in each mutant strain. This caused the control and *aps3*Δ/Δ strains to grow exclusively as extended hyphae (Fig. 5A). The *vps21*Δ/Δ mutant formed marginally

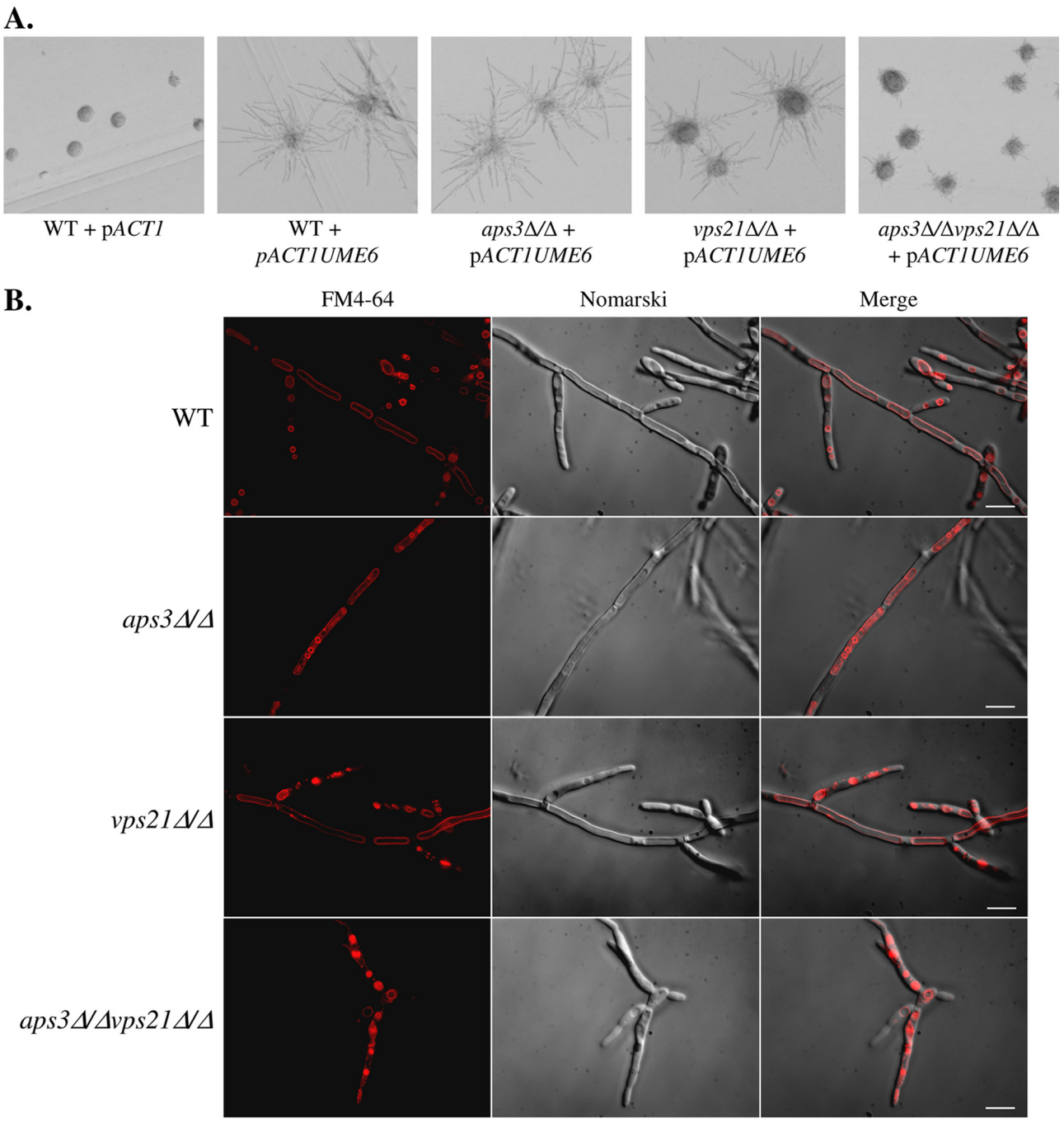

FIG. 5. Overexpression of *UME6* does not restore normal hyphal elongation to the *aps3*Δ/Δ *vps21*Δ/Δ mutant. *UME6* was overexpressed from the *ACT1* promoter in CAI4 ("wild-type" [WT] control), *aps3*Δ/Δ, *vps21*Δ/Δ, and *aps3*Δ/Δ *vps21*Δ/Δ strain backgrounds. Each strain was also transformed with the p*ACT1* vector alone (shown only for the control strain). (A) Strains were streaked to YPD and grown at 30°C. (B) Each strain was grown in YPD broth at 30°C, stained with FM4-64, and observed using a deconvolution microscope. Scale bar, 10 μM.

less-elongated hyphae, while the hyphae formed in the *aps3*Δ/Δ*vps21*Δ/Δ background were dramatically shorter than those of the control. Thus, normal hyphal growth cannot be restored in the *vps21*Δ/Δ and *aps3*Δ/Δ *vps21*Δ/Δ strains by overexpression of Ume6p. Rim101p is a pH-responsive transcription factor required for alkaline-induced hyphal growth (14, 15). Defects in Rim101p activation have been shown to contribute to the hyphal growth defects in several *C. albicans* endosomal trafficking mutants (25, 46). However, introduction of a "dominant active" *RIM101* allele (15) also failed to restore normal hyphal growth in the *vps21*Δ/Δ (23) or *aps3*Δ/Δ *vps21*Δ/Δ mutants (data not shown).

Finally, it has been shown previously that a *vma7*Δ/Δ mutant, lacking a subunit of the vacuolar v-ATPase, has defects in hyphal growth and virulence (37), presumably due to an inability to acidify its vacuole. Thus, it was considered that a

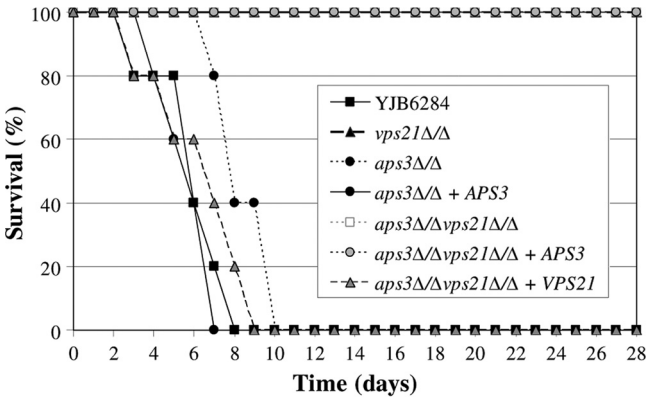

FIG. 6. Vps21p-mediated trafficking is of greater significance to pathogenesis than Aps3p-mediated trafficking. Five BALB/c mice were inoculated intravenously with approximately 5×10^5 cells of each *C. albicans* strain. Survival curves were plotted for a 28-day period. Note that the survival curves of *vps21*Δ/Δ, *aps3*Δ/Δ *vps21*Δ/Δ, and *aps3*Δ/Δ *vps21*Δ/Δ plus *APS3* strains overlap. A repeat experiment was performed with three additional mice per strain, with similar results.

block in vacuolar trafficking of the v-ATPase may account for the defective hyphal growth in the *aps3*Δ/Δ *vps21*Δ/Δ mutant. However, unlike the *vma7*Δ/Δ mutant, *aps3*Δ/Δ, *vps21*Δ/Δ, and *aps3*Δ/Δ *vps21*Δ/Δ mutants were all able to grow at pH 8 (Fig. 3A) and accumulated the weak base quinacrine within their vacuoles (data not shown). These data suggest that acidification of the vacuoles in each mutant was unaffected.

Overexpression of *UME6* induces hyphal growth with vacuolated subapical cells. *C. albicans* hyphal growth involves the induction of a hypha-specific transcription program, as well as posttranslational modulation of proteins to establish a polarized, or apical mode of growth. However, it is unknown how subapical vacuolation is coordinated with these events. To examine the interrelationship between hypha-specific transcriptional responses and subapical vacuolation, vacuole morphology was examined in the *UME6* overexpression strains. Strains were grown in YPD medium at 30°C, and vacuoles were labeled with FM4-64. In the wild-type background, the elongated hyphae induced by *UME6* overexpression had extensively vacuolated subapical compartments (Fig. 5B). Cell compartments near the hyphal tip had much smaller, rounder compartments labeled with FM4-64. This demonstrates that *UME6* overexpression is sufficient to induce hyphal growth with subapical vacuolation. Like the control strain, the *aps3*Δ/Δ and *vps21*Δ/Δ mutants also formed hyphae with extensively vacuolated subapical compartments, except that the *aps3*Δ/Δ mutant had multiple intravacuolar vesicles, as seen in the yeast form. However, the double mutant formed only pseudohyphae with spherical vacuoles (similar to those seen in the yeast form) and many cells with highly fragmented vacuoles (33.5%; $n = 200$).

***APS3* and *VPS21* make additive contributions to *C. albicans* pathogenesis.** The virulence of each mutant was tested in a mouse model of disseminated candidiasis. The *aps3*Δ/Δ mutant was fully virulent, causing 100% mortality (Fig. 6). In a previous report the *vps21*Δ/Δ mutant had significantly reduced virulence in this model (23), causing 50% mortality over 28 days. In this study all *vps21*Δ/Δ mutant-infected mice survived, but each exhibited symptoms, including fur ruffling. The *aps3*Δ/Δ *vps21*Δ/Δ double mutant was completely avirulent, with all infected mice surviving and exhibiting no obvious symptoms. Reintroduction of *APS3* to the double mutant restored fur ruffling but not the capacity to cause mortality, while reintroducing *VPS21* restored mortality. Finally, the fungal burden within the kidneys of mice surviving to day 28 was determined. The *aps3*Δ/Δ *vps21*Δ/Δ mutant was not detected in kidney tissue, suggesting that it is cleared from the inoculated mice. However, while neither *vps21*Δ/Δ or *aps3*Δ/Δ *vps21*Δ/Δ plus *APS3* strains caused lethal infection, both were able to persist within the kidney tissue at significant levels ($5.5 \times 10^5 \pm 5.1 \times 10^5$ and $6.8 \times 10^5 \pm 5.7 \times 10^5$ CFU g^{-1}, respectively; mean ± standard deviation [SD]; $n = 5$). This suggests that *APS3*-dependent trafficking does play a role in *C. albicans* pathogenesis in the absence of *VPS21*-mediated transport.

DISCUSSION

Previous studies have clearly established that disruption of vacuolar trafficking leads to defective hyphal growth and loss of virulence in *C. albicans* (8, 23, 35). However, the specific trafficking events required for each of these processes are unknown. This study has established that *C. albicans* has an AP-3-dependent vacuolar trafficking pathway. Deletion of *APS3* led to the accumulation of large vesicles within the vacuole lumens of many cells, which could be explained by a deficiency in the breakdown of multivesicular bodies or autophagosomes. The Vps21p Rab GTPase was previously localized to the late endosome and has an established role in vacuolar trafficking (23). The distinct vacuolar morphology and stress phenotypes of the *aps3*Δ/Δ and *vps21*Δ/Δ mutants suggest that Aps3p and Vps21p operate in distinct trafficking pathways to the *C. albicans* vacuole, as is the case in *S. cerevisiae*. In support of this, the Mlt1-GFP fusion protein localized to the vacuolar membrane in either single mutant but showed significant mislocalization in the double mutant. This suggests that the Mlt1p "cargo" can transit to the vacuole via either Aps3p- or Vps21p-mediated pathways. Nonetheless, despite disruption of both AP-3 and endosomal trafficking routes, a significant amount of Mlt1-GFP reached the vacuole, and the *aps3*Δ/Δ *vps21*Δ/Δ mutant had a largely intact vacuole compartment. Furthermore, the modest reduction in ALP activity and normal vacuolar acidification suggest that additional trafficking routes may exist between the Golgi apparatus and vacuole in *C. albicans*.

Initial phenotypic analyses of the *aps3*Δ/Δ mutant failed to identify any substantial defect in stress resistance or polarized hyphal growth. This suggested that the ALP trafficking pathway was of little consequence in *C. albicans*. In addition to the mild stress phenotypes and increased protease secretion previously reported (23), the *vps21*Δ/Δ mutant was also found to be sensitive to agents which disrupt cell wall integrity. These phenotypes are consistent with those reported by Lee and colleagues (27), and they suggest that disrupting endosomal transport may influence secretion and cell surface composition. Loss of Aps3p had no effect on secretion, endocytosis, or cell wall integrity. Interestingly, loss of both genes resulted in synthetic stress phenotypes. This further supports the notion that Aps3p and Vps21p operate in distinct pathways which share some functional overlap.

While the loss of *APS3* has little impact upon hyphal growth,

loss of *APS3* in the *vps21*Δ/Δ background has a profound impact. The double mutant grows at an essentially normal rate in the yeast form; thus, this is not merely the result of reduced growth-limiting apical extension. This suggests that Golgi-to-vacuole transport via Aps3p- and Vps21p-dependent routes is particularly important during polarized hyphal growth. Ume6p overexpression enabled us to induce constitutive hyphal growth in a rich medium at 30°C, stress-free conditions under which all strains grow at similar rates in the yeast form. Ume6p overexpression was sufficient to induce hyphal growth with vacuolated subapical cells in the wild-type, *aps3*Δ/Δ, and *vps21*Δ/Δ backgrounds. This distribution of vacuoles is similar to that described by Gow and colleagues for *C. albicans* grown under hypha-inducing conditions (21). However, the double mutant formed only pseudohyphae with spherical (similar to those observed in yeast cells) or fragmented vacuoles. These data are consistent with the double mutant being unable to facilitate the dynamic changes in vacuolar trafficking required to support true hyphal growth. It also suggests that Golgi-to-vacuole trafficking through either the AP-3 or the endosomal route is sufficient to support subapical vacuole expansion during polarized hyphal growth.

Several previously described *C. albicans* mutants with disrupted vacuole morphology have profound defects in hyphal growth. Despite an apparently normal-sized vacuole compartment, the *aps3*Δ/Δ *vps21*Δ/Δ mutant exhibited profound defects in hyphal growth. Eck and colleagues have also reported a *vps34*Δ/Δ mutant with defects in vacuolar trafficking (8). The *vps34*Δ/Δ mutant had an enlarged vacuole in the yeast form but still has severely reduced hyphal growth. These results suggest that a controlled flow of membrane between the Golgi apparatus and vacuole is required to support hyphal growth, rather than an intact vacuole morphology *per se*. The *UME6* overexpression data imply that the mechanisms responsible for subapical vacuole expansion lie downstream of Ume6p and are controlled either directly or indirectly by hypha-specific transcriptional responses. To my knowledge, this provides the first link between hypha-specific signaling and control of vacuolar dynamics in *C. albicans*. Putting these data together suggests a simple model where activation of the transcription factor Ume6p stimulates Golgi-to-vacuole transport to promote subapical vacuole expansion. Thus, overexpression of a single regulator of hyphal growth, Ume6p, is sufficient to induce both an apical mode of growth and subapical vacuolation. This suggests that these processes may be coregulated.

Vacuolar trafficking may support hyphal growth through several possible mechanisms. First, it seems likely that disruption of vacuolar trafficking would prevent vacuolation of subapical cells, and this may limit hyphal elongation. Second, the vacuole has an established role in regulating turgor pressure within the fungal cell (24), which may help support hyphal extension by providing a force for directional growth (30). Thus, defective regulation of turgor pressure in vacuolar mutants may limit apical extension. Finally, it is possible that a specific "factor" is required to localize to the vacuole to support polarized hyphal growth. For example, loss of the vacuolar v-ATPase subunit Vma7p (and consequently vacuolar acidification) results in defective hyphal growth (37). However, vacuolar acidification was apparently intact in the *aps3*Δ/Δ *vps21*Δ/Δ mutant. Nonetheless, other factors required for hyphal growth may be prevented from reaching the vacuole.

Loss of *APS3* had no obvious impact on *C. albicans* virulence in the mouse model of disseminated candidiasis, while loss of *VPS21* resulted in a dramatic reduction in virulence. However, the *vps21*Δ/Δ mutant is clearly able to persist within host kidney tissue, while the *aps3*Δ/Δ *vps21*Δ/Δ mutant was not. This again suggests that the Aps3p-dependent route has a minor role in virulence, but this becomes more significant when Vps21p trafficking is blocked.

In conclusion, *APS3* affects vacuolar trafficking through a pathway which is distinct from the *VPS21*-mediated endosomal route. Furthermore, Aps3p-dependent trafficking to the vacuole plays a minor role in supporting *C. albicans* hyphal growth and virulence, with this role especially important when endosomal trafficking is disrupted. These results also suggest that there may be additional pathways which operate between the Golgi apparatus and the vacuole in *C. albicans*. Defining which vacuolar functions and pathways are required for pathogenesis will be crucial to devise new strategies which exploit this organelle for therapeutic intervention.

ACKNOWLEDGMENTS

This publication was made possible by grant number P20RR020160 from the National Center for Research Resources (NCRR), a component of the National Institutes of Health (NIH).

The contents of this publication are solely the responsibility of the author and do not necessarily represent the official view of NCRR or NIH.

I thank Aaron Mitchell (Carnegie Mellon University), William Fonzi (Georgetown University), Fritz Muhlschlegel (University of Kent), and Alistair Brown (University of Aberdeen) for strains and plasmid constructs. Special thanks to Rebecca Fitch from the LSUHSC Gene Therapy Program's Morphology and Imaging Core for assistance with imaging.

REFERENCES

1. **Banerjee, M., D. S. Thompson, A. Lazzell, P. L. Carlisle, C. Pierce, C. Monteagudo, J. L. Lopez-Ribot, and D. Kadosh.** 2008. *UME6*, a novel filament-specific regulator of *Candida albicans* hyphal extension and virulence. Mol. Biol. Cell **19:**1354–1365.
2. **Barelle, C. J., E. A. Bohula, S. J. Kron, D. Wessels, D. R. Soll, A. Schafer, A. J. Brown, and N. A. Gow.** 2003. Asynchronous cell cycle and asymmetric vacuolar inheritance in true hyphae of *Candida albicans*. Eukaryot. Cell **2:**398–410.
3. **Bensen, E. S., S. G. Filler, and J. Berman.** 2002. A Forkhead transcription factor is important for true hyphal as well as yeast morphogenesis in *Candida albicans*. Eukaryot. Cell **1:**787–798.
4. **Bernardo, S. M., Z. Khalique, J. Kot, J. K. Jones, and S. A. Lee.** 2008. *Candida albicans VPS1* contributes to protease secretion, filamentation, and biofilm formation. Fungal Genet. Biol. **45:**861–877.
5. **Boeke, J. D., F. LaCroute, and G. R. Fink.** 1984. A positive selection for mutants lacking orotidine-5′-phosphate decarboxylase activity in yeast: 5-fluoro-orotic acid resistance. Mol. Gen. Genet. **197:**345–346.
6. **Bowers, K., and T. H. Stevens.** 2005. Protein transport from the late Golgi to the vacuole in the yeast *Saccharomyces cerevisiae*. Biochim. Biophys. Acta **1744:**438–454.
7. **Brown, D. H., Jr., A. D. Giusani, X. Chen, and C. A. Kumamoto.** 1999. Filamentous growth of *Candida albicans* in response to physical environmental cues and its regulation by the unique *CZF1* gene. Mol. Microbiol. **34:** 651–662.
8. **Bruckmann, A., W. Kunkel, A. Hartl, R. Wetzker, and R. Eck.** 2000. A phosphatidylinositol 3-kinase of *Candida albicans* influences adhesion, filamentous growth and virulence. Microbiology **146**(Pt. 11)**:**2755–2764.
9. **Bryant, N. J., and T. H. Stevens.** 1998. Vacuole biogenesis in *Saccharomyces cerevisiae*: protein transport pathways to the yeast vacuole. Microbiol. Mol. Biol. Rev. **62:**230–247.
10. **Burke, D., D. Dawson, and T. Stearns.** 2000. Methods in yeast genetics: a Cold Spring Harbor Laboratory course manual. Cold Spring Harbor Laboratory Press, Cold Spring Harbor, NY.
11. **Carlisle, P. L., M. Banerjee, A. Lazzell, C. Monteagudo, J. L. Lopez-Ribot,**

and D. Kadosh. 2009. Expression levels of a filament-specific transcriptional regulator are sufficient to determine *Candida albicans* morphology and virulence. Proc. Natl. Acad. Sci. U. S. A. **106:**599–604.
12. **Cowles, C. R., G. Odorizzi, G. S. Payne, and S. D. Emr.** 1997. The AP-3 adaptor complex is essential for cargo-selective transport to the yeast vacuole. Cell **91:**109–118.
13. **Crandall, M., and J. E. Edwards, Jr.** 1987. Segregation of proteinase-negative mutants from heterozygous *Candida albicans*. J. Gen. Microbiol. **133**(Pt. 10)**:**2817–2824.
14. **Davis, D., R. B. Wilson, and A. P. Mitchell.** 2000. *RIM101*-dependent and -independent pathways govern pH responses in *Candida albicans*. Mol. Cell. Biol. **20:**971–978.
15. **El Barkani, A., O. Kurzai, W. A. Fonzi, A. Ramon, A. Porta, M. Frosch, and F. A. Muhlschlegel.** 2000. Dominant active alleles of *RIM101* (*PRR2*) bypass the pH restriction on filamentation of *Candida albicans*. Mol. Cell. Biol. **20:**4635–4647.
16. **Fernandes, J., R. Amorim, I. Azevedo, and M. J. Martins.** 2008. In vitro modulation of alkaline phosphatase activity of *Saccharomyces cerevisiae* grown in low or high phosphate medium. Braz. J. Med. Biol. Res. **41:**41–46.
17. **Gerami-Nejad, M., J. Berman, and C. A. Gale.** 2001. Cassettes for PCR-mediated construction of green, yellow, and cyan fluorescent protein fusions in *Candida albicans*. Yeast **18:**859–864.
18. **Gerrard, S. R., N. J. Bryant, and T. H. Stevens.** 2000. *VPS21* controls entry of endocytosed and biosynthetic proteins into the yeast prevacuolar compartment. Mol. Biol. Cell **11:**613–626.
19. **Gietz, D., A. St. Jean, R. A. Woods, and R. H. Schiestl.** 1992. Improved method for high efficiency transformation of intact yeast cells. Nucleic Acids Res. **20:**1425.
20. **Gillum, A. M., E. Y. Tsay, and D. R. Kirsch.** 1984. Isolation of the *Candida albicans* gene for orotidine-5′-phosphate decarboxylase by complementation of *S. cerevisiae ura3* and *E. coli pyrF* mutations. Mol. Gen. Genet. **198:**179–182.
21. **Gow, N. A., and G. W. Gooday.** 1982. Vacuolation, branch production and linear growth of germ tubes in *Candida albicans*. J. Gen. Microbiol. **128:** 2195–2198.
22. **Guthrie, C., and G. Fink.** 1991. Guide to yeast genetics and molecular biology. Academic Press, New York, NY.
23. **Johnston, D. A., K. E. Eberle, J. E. Sturtevant, and G. E. Palmer.** 2009. Role for endosomal and vacuolar GTPases in *Candida albicans* pathogenesis. Infect. Immun. **77:**2343–2355.
24. **Klionsky, D. J., P. K. Herman, and S. D. Emr.** 1990. The fungal vacuole: composition, function, and biogenesis. Microbiol. Rev. **54:**266–292.
25. **Kullas, A. L., M. Li, and D. A. Davis.** 2004. Snf7p, a component of the ESCRT-III protein complex, is an upstream member of the *RIM101* pathway in *Candida albicans*. Eukaryot. Cell **3:**1609–1618.
26. **Lay, J., L. K. Henry, J. Clifford, Y. Koltin, C. E. Bulawa, and J. M. Becker.** 1998. Altered expression of selectable marker *URA3* in gene-disrupted *Candida albicans* strains complicates interpretation of virulence studies. Infect. Immun. **66:**5301–5306.
27. **Lee, S. A., J. Jones, Z. Khalique, J. Kot, M. Alba, S. Bernardo, A. Seghal, and B. Wong.** 2007. A functional analysis of the *Candida albicans* homolog of *Saccharomyces cerevisiae VPS4*. FEMS Yeast Res. **7:**973–985.
28. **Lo, H. J., J. R. Kohler, B. DiDomenico, D. Loebenberg, A. Cacciapuoti, and G. R. Fink.** 1997. Nonfilamentous *C. albicans* mutants are avirulent. Cell **90:**939–949.
29. **Merson-Davies, L. A., and F. C. Odds.** 1989. A morphology index for characterization of cell shape in *Candida albicans*. J. Gen. Microbiol. **135:**3143–3152.
30. **Money, N.** 1997. Wishful thinking of turgor revisited: the mechanics of hyphal growth. Fungal Genet. Biol. **21:**173–187.
31. **Murad, A. M., P. R. Lee, I. D. Broadbent, C. J. Barelle, and A. J. Brown.** 2000. CIp10, an efficient and convenient integrating vector for *Candida albicans*. Yeast **16:**325–327.
32. **Noda, T., J. Kim, W. P. Huang, M. Baba, C. Tokunaga, Y. Ohsumi, and D. J. Klionsky.** 2000. Apg9p/Cvt7p is an integral membrane protein required for transport vesicle formation in the Cvt and autophagy pathways. J. Cell Biol. **148:**465–480.
33. **Odds, F. C., L. Van Nuffel, and N. A. Gow.** 2000. Survival in experimental *Candida albicans* infections depends on inoculum growth conditions as well as animal host. Microbiology **146**(Pt. 8)**:**1881–1889.
34. **Palmer, G. E., A. Cashmore, and J. Sturtevant.** 2003. *Candida albicans VPS11* is required for vacuole biogenesis and germ tube formation. Eukaryot. Cell **2:**411–421.
35. **Palmer, G. E., M. N. Kelly, and J. E. Sturtevant.** 2005. The *Candida albicans* vacuole is required for differentiation and efficient macrophage killing. Eukaryot. Cell **4:**1677–1686.
36. **Palmer, G. E., and J. E. Sturtevant.** 2004. Random mutagenesis of an essential Candida albicans gene. Curr. Genet. **46:**343–356.
37. **Poltermann, S., M. Nguyen, J. Gunther, J. Wendland, A. Hartl, W. Kunkel, P. F. Zipfel, and R. Eck.** 2005. The putative vacuolar ATPase subunit Vma7p of *Candida albicans* is involved in vacuole acidification, hyphal development and virulence. Microbiology **151:**1645–1655.
38. **Ramon, A. M., and W. A. Fonzi.** 2003. Diverged binding specificity of Rim101p, the *Candida albicans* ortholog of PacC. Eukaryot. Cell **2:**718–728.
39. **Saville, S. P., A. L. Lazzell, C. Monteagudo, and J. L. Lopez-Ribot.** 2003. Engineered control of cell morphology in vivo reveals distinct roles for yeast and filamentous forms of *Candida albicans* during infection. Eukaryot. Cell **2:**1053–1060.
40. **Stepp, J. D., K. Huang, and S. K. Lemmon.** 1997. The yeast adaptor protein complex, AP-3, is essential for the efficient delivery of alkaline phosphatase by the alternate pathway to the vacuole. J. Cell Biol. **139:**1761–1774.
41. **Theiss, S., M. Kretschmar, T. Nichterlein, H. Hof, N. Agabian, J. Hacker, and G. A. Kohler.** 2002. Functional analysis of a vacuolar ABC transporter in wild-type *Candida albicans* reveals its involvement in virulence. Mol. Microbiol. **43:**571–584.
42. **Veses, V., A. Richards, and N. A. Gow.** 2009. Vacuole inheritance regulates cell size and branching frequency of *Candida albicans* hyphae. Mol. Microbiol. **71:**505–519.
43. **Vida, T. A., and S. D. Emr.** 1995. A new vital stain for visualizing vacuolar membrane dynamics and endocytosis in yeast. J. Cell Biol. **128:**779–792.
44. **Wilson, R. B., D. Davis, B. M. Enloe, and A. P. Mitchell.** 2000. A recyclable *Candida albicans URA3* cassette for PCR product-directed gene disruptions. Yeast **16:**65–70.
45. **Wilson, R. B., D. Davis, and A. P. Mitchell.** 1999. Rapid hypothesis testing with *Candida albicans* through gene disruption with short homology regions. J. Bacteriol. **181:**1868–1874.
46. **Xu, W., F. J. Smith, Jr., R. Subaran, and A. P. Mitchell.** 2004. Multivesicular body-ESCRT components function in pH response regulation in *Saccharomyces cerevisiae* and *Candida albicans*. Mol. Biol. Cell **15:**5528–5537.